*J. Physiol.* (1978), **284**, *pp.* 155–179
*With* 15 *text-figures*
*Printed in Great Britain*



# CRAYFISH STRETCH RECEPTOR: AN INVESTIGATION WITH VOLTAGE-CLAMP AND ION-SENSITIVE ELECTRODES

BY H. MACK BROWN, DAVID OTTOSON AND BO RYDQVIST

*From the Department of Physiology, University of Utah Research Park, Salt Lake City, Utah 84108, U.S.A. and the Department of Physiology, Karolinska Institutet, Stockholm, Sweden*

(*Received 13 March 1978*)

SUMMARY

1. The membrane characteristics of the slowly adapting stretch receptor from the crayfish, *Astacus fluviatilis*, were examined with electrophysiological techniques consisting of membrane potential recording, voltage clamp and ion-sensitive microelectrodes.

2. The passive membrane current ($I_p$) following step changes of the membrane potential to levels above 0 mV required more than a minute to decay to a steady-state level.

3. The stretch-induced current (*SIC*, where $SIC = I_{total} - I_{passive}$) was not fully developed until the $I_p$ had decayed to a steady state.

4. With $I_p$ at the steady state and the stretch-induced current at the 0-current potential, a slow stretch-induced inward current was isolated. The latter reaches a maximum after 1 sec of stretch and declines even more slowly after stretch. The $I$–$V$ relation of the slow current had a negative slope and reversed sign near the resting potential. It is suggested that this current is due to a $Cl^-$ conductance change.

5. The stretch-induced current, consisting of a rapid transient phase and a steady component can be isolated from the slow stretch-induced current at a holding potential corresponding to the resting potential.

6. The $SIC$–$E_m$ relation is non-linear and reverses sign at about +15 mV.

7. In a given cell, the reversal potential of the stretch-induced potential change obtained with current clamp coincided with the 0-current potential of the stretch-induced current obtained by voltage clamp. The average value from twenty-six cells was $+13 \pm 6{\cdot}5$ mV; cell to cell variability seemed to be correlated with dendrite length.

8. Tris (mol. wt. 121) or arginine (mol. wt. 174) substituted for $Na^+$ reduces but does not abolish the stretch-induced current.

9. The permeability ratios of Tris : Na and arginine : Na were estimated from changes in the 0-current potential as these cations replaced $Na^+$ in the exernal medium. The $P_{Tris}:P_{Na}$ was somewhat higher (0·31) than the $P_{arginine}:P_{Na}$ ratio (0·25).

10. Changes in the external $Ca^{2+}$ concentration had no effect on the 0-current potential in Na or Tris saline. However, reducing $Ca^{2+}$ did augment the stretch-induced current in either saline. A tenfold reduction of $Ca^{2+}$ increased the conductance (at the 0-current level) about twofold.

11. Intracellular $K^+$ and $Cl^-$ activities were obtained with ion sensitive electrodes. The average values from six cells were $a^i_K = 133 \pm 34$ mM and $a^i_{Cl} = 15{\cdot}2 \pm 1{\cdot}8$ mM S.D.). $E_K$ was about 20 mV more negative than $E_m$ and $E_{Cl}$ was about 10 mV more positive than $E_m$.

12. $a^i_K$ and resting $E_m$ undergo large changes in $K^+$-free solutions. After 60 min, $a^i_K$ was reduced eightfold and $E_m$ was reduced from $-67$ to $-40$ mV. Reduced $Ca^{2+}$ in $K^+$-free augments the rate of these changes. Receptor potential amplitude was also reduced in $K^+$-free solution but could be restored upon polarizing the membrane to the pre-existing resting level.

## INTRODUCTION

Investigations of receptor mechanisms with the voltage clamp technique have provided new information concerning the ionic mechanisms involved in production of the receptor potential. To date most of this work has been conducted on large invertebrate photoreceptors (see for example, Millecchia & Mauro, 1969; Hagiwara, Koike & Meech, 1970; Brown & Mote, 1974). Only one investigation utilizing this technique has been reported on the stretch receptor of crayfish (Klie & Wellhöner, 1973).

The present study was conducted to attempt to quantify more thoroughly the involvement of different ions in the production of the receptor potential of the crayfish stretch receptor and to make intracellular measurements of $Cl^-$ and $K^+$ with ion-specific electrodes. An early study on this receptor utilizing a single microelectrode and methods of ion replacement provided the important conclusion tha $Na^+$ was principally involved in the receptor potential (Edwards, Terzuolo & Washizu, 1963), but left unanswered the role of other ions including $Ca^{2+}$. Membrane polarization and recording with two micro-electrodes (Obara, 1968) provided additional information concerning changes of passive membrane conductance during ion substitution and the voltage clamp provided for the first time an accurate estimate of the reversal potential in normal saline (Klie & Wellhöner, 1973). Klie & Wellhöner's measurements indicated that the reversal potential was on the average about +25 mV and even though considerable variation was observed from cell to cell, only four of twenty-five cells had reversal potentials between 0 and +5 mV. Previous estimates had ranged from $-30$ mV (Obara, 1968) to 0 mV (Terzuolo & Washizu, 1962).

The present investigation extends these observations and provides new information concerning additional components of membrane current that contribute to the receptor potential. In addition, estimates of the equilibrium potential for $Cl^-$ and $K^+$ were obtained by measuring intracellular $K^+$ and $Cl^-$ activities with ion exchanger electrodes. This enables a definite estimate of two important ionic batteries in this cell. $K^+$ electrodes were also used to evaluate the effects of $K^+$-free and $K^+$-free, $Ca^{2+}$-free solutions on intracellular $K^+$. These studies were conducted to compare possible mechanisms for the changes in the receptor potential which have been described in the stretch receptor and the muscle spindle (cf. Husmark & Ottoson, 1971; Ottoson & Husmark, 1971).

## METHODS

The experiments were carried out on the slowly adapting stretch receptor of the crayfish (*Astacus fluviatilis*). The receptor neurone with its muscle were isolated from the second or the

third abdominal segment of the crayfish and mounted in a small chamber filled with saline. The temperature of the bath was maintained at +15 °C by means of a peltier device.

The general arrangement of the experimental set-up is illustrated schematically in Fig. 1. The ends of the receptor muscle were tied firmly to a thin tungsten rod (0·1 mm) which passed through a glass capillary and thence to a Brush pen motor with position and velocity feed-back controls. The neurone was placed on a small platform of glass while the muscle passed freely through the bathing fluid to the attachments on the tungsten rods. Dark-field microscopy was chosen to place the electrodes and to make the neurone clearer.

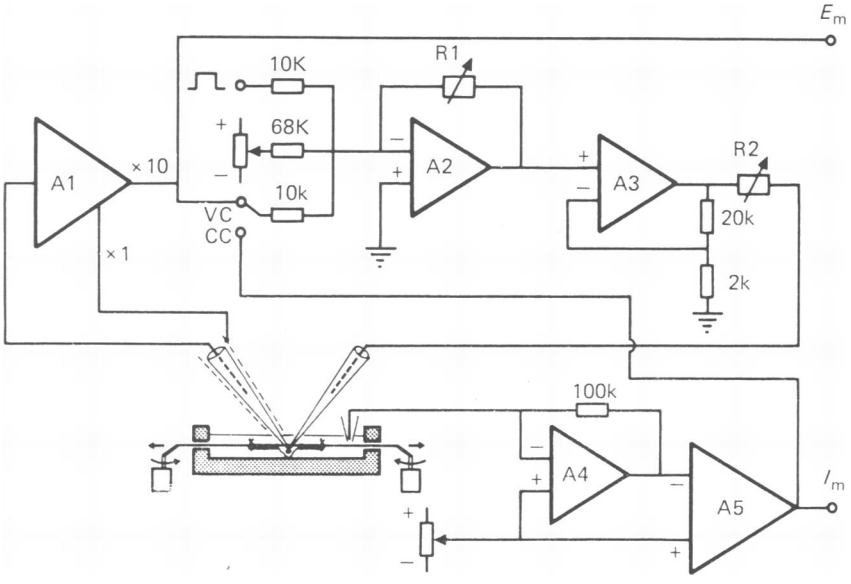


Fig. 1. Schematic representation of experimental arrangement for recording membrane potential and voltage clamp of stretch receptor neuron. Neurone maintained in same position by asymmetric stretch applied by two pen motors adjacent to recording chamber. Left internal micro-electrode: to record potential difference between it and an agar-KCl electrode in the bath (on right). Right internal electrode: to pass current between it and bath electrode. A1: unity-gain capacity compensated probe. VC: voltage clamp; CC: current clamp. Command signal, holding potential and $E_m$ signal fed to variable-gain, summing amplifier A2 (Burr-Brown 3341/15C). A3: power amplifier (Burr-Brown 3582). A4: current to voltage transducer. A5: to nullify the effect of bucking potential on A4.

*Stretching apparatus*

The neurone was stretched by applying pulses of different wave forms to the Brush pen motors. The applied stretch was generally a ramp-and-hold of various durations. The position feed-back signals to the pen motors were used to record displacement. Before impalement of the neurone, the stretch applied to each end of the muscle was adjusted so that the cell body remained in the same position during stretch as during rest. In this way it was possible to avoid electrode artifacts and dislodgement of the electrodes during stretching. This method worked very reliably since experiments could be conducted with repeated test stretches over several hours after the initial penetration with the electrodes.

*Ion-sensitive micro-electrodes*

Liquid ion-exchanger (Corning exchanger 477317 and 477315) micro-electrodes were constructed to measure $K^+$ and $Cl^-$ activities (Brown, 1976). Internal $Cl^-$ activity was also measured in a few experiments with Ag/AgCl micro-electrodes as described by Saunders & Brown (1977). No correction for interference from intracellular ions was made in the present study.

*Determination of internal ion activity* ($a_x^i$)

The ion-sensitive electrode was connected via Ag/AgCl wires to a FET amplifier (Burr-Brown 3522). The signal was displayed together with the membrane potential on a chart recorder. The signals were also subtracted electrically so that the potential difference ($V_I^i - E_m$) could be used to calculate the internal ion activity ($a_x^i$; = $K^+$ or $Cl^-$) from the relation

$$a_x^i = a_x^o . \exp \frac{(V_I^i - E_m - V_I^o}{m} \quad (1)$$

TABLE 1. Composition of salines (mM)

| | NaCl | KCl | $CaCl_2$ | $MgCl_2$ | Tris | Arginine, HCl |
|---|---|---|---|---|---|---|
| Normal *Astacus* saline (NAS) | 210 | 5·4 | 13·5 | 1·2 | 10 | — |
| Na-free (Tris) | — | 5·4 | 13·5 | 1·2 | 230 | — |
| Na-free (arginine) | — | 5·4 | 13·5 | 1·2 | 10 | 210 |
| Na-free (Tris), Ca-free (Mg) | — | 5·4 | — | 14·7 | 230 | — |
| K-free (Na) | 215 | — | 13·5 | 1·2 | 10 | — |
| K-free (Na), Ca-free (Mg) | 215 | — | — | 14·7 | 10 | — |

pH = 7·3.

where $V_I^o$ is the potential of the ion electrode in the external solution with primary ion activity $a_x^o$; $V_I^i$ is the potential of the ion electrode inside the cell; $m$ is $dV/da_x$ of the ion sensitive electrode after calibration in pure solutions of the primary ion $x$.

*Solutions*

The composition of the solutions is given in Table 1. Ions in parentheses indicate the ion substituted for the principal ion. The solutions were buffered with Tris to pH 7·2–7·4.

*Membrane potential recording and voltage-clamp technique*

The neurone was impaled under visual control with two glass micropipettes filled with 3 M-KCl (resistance 5–10 MΩ). Membrane potential was recorded as the potential difference between an intracellular micropipette and an agar-KCl Ag/AgCl electrode in the bath. The second intracellular electrode was used to pass constant current pulses across the membrane or to control the membrane potential by the feed-back circuit shown in Fig. 1. The potential recording micropipette was shielded and the shield was driven from the output of the probe. The time required to clamp the membrane potential to a final value with the system used was about 0·5 msec when a rectangular commanding voltage pulse was applied. Membrane current was measured as the voltage drop across the feed-back resistor of A4 which held the saline bath at ground potential. The membrane potential ($E_m$), the membrane current ($I_m$) and the stretch wave form and amplitude were displayed on a CRO and a chart recorder. The signals were also fed to a 4-channel tape recorder (Hewlett Packard 3960). Resting membrane potential was measured with the receptor muscle kept at resting length. Ramp and hold stretches were usually 1·2–1·4 sec long. During voltage-clamp, the membrane potential was usually shifted to a positive potential value of about +40 mV and measurements were made when membrane current was in the steady state. From this potential value the potential was changed in steps of about −10 mV and test stretches applied at each potential level.

## RESULTS

### *Current clamp*

The values of the reversal potential for the stretch-induced potential change obtained with current clamp were of interest because of the wide range of values reported in the literature and because no experimental records have appeared showing reversal of the stretch-induced potential change with current clamp.

The traces shown in the inset of Fig. 2 were obtained by polarizing the membrane with current from an intracellular KCl-filled micro-electrode until a steady-state $E_m$ was obtained before applying the stretch. By shifting the membrane potential to large positive values and then stepping down the current after a stretch-induced potential change, reproducible values of the reversal potential could be obtained. At

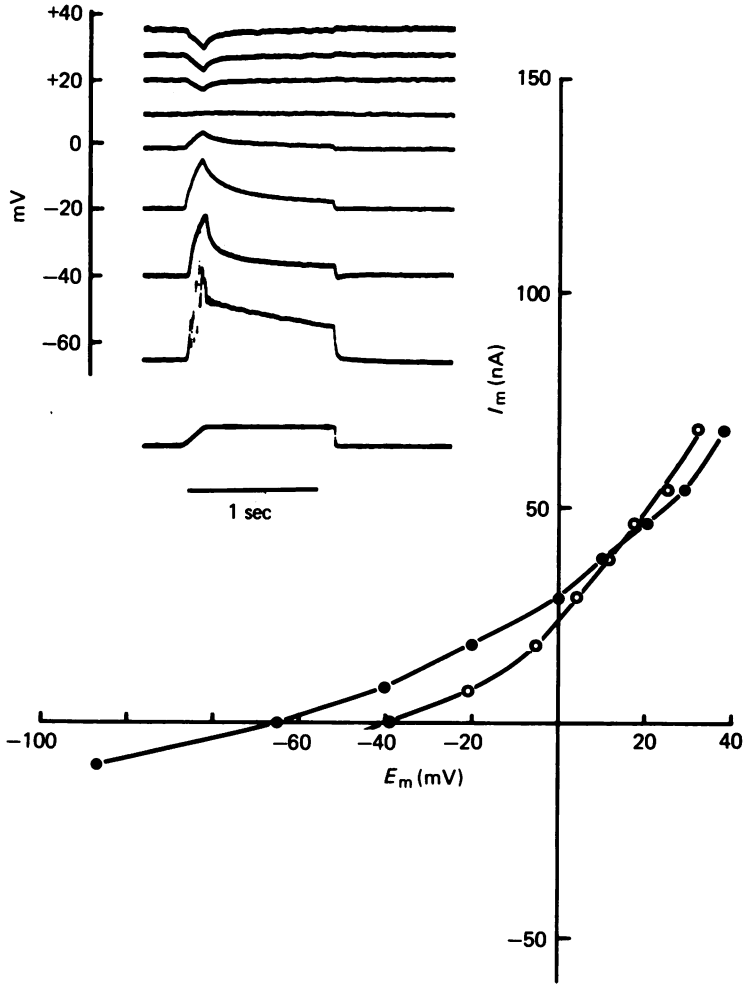


Fig. 2. Inset: change in stretch-induced potential at different membrane potential ($E_m$) levels preset to a constant level by passing current across the membrane.

*I–V* curves from data shown in the inset. Filled circles represent steady-state $E_m$ obtained from a given amount of current. Open symbols represent the peak $E_m$ obtained during stretch at the same current level.

the most positive membrane potential ( +37·5 mV), the potential change obtained from stretch consisted of a negative-going peak and steady phase. As the membrane potential was subsequently shifted to more negative values, a membrane potential value was reached at which stretch produced no potential change with these features (reversal potential). This was about +13 mV in the cell shown in Fig. 1. At more negative values of $E_m$ than the reversal potential, the stretch-induced potential

change consisted of a positive peak and steady phase and the amplitude increased as the membrane potential was shifted toward the resting potential (−65 mV). Action potentials noted on the stretch-induced potential change at the resting potential were absent in the other traces due to inactivation of the $Na^+$ current produced by the more positive membrane potential values.

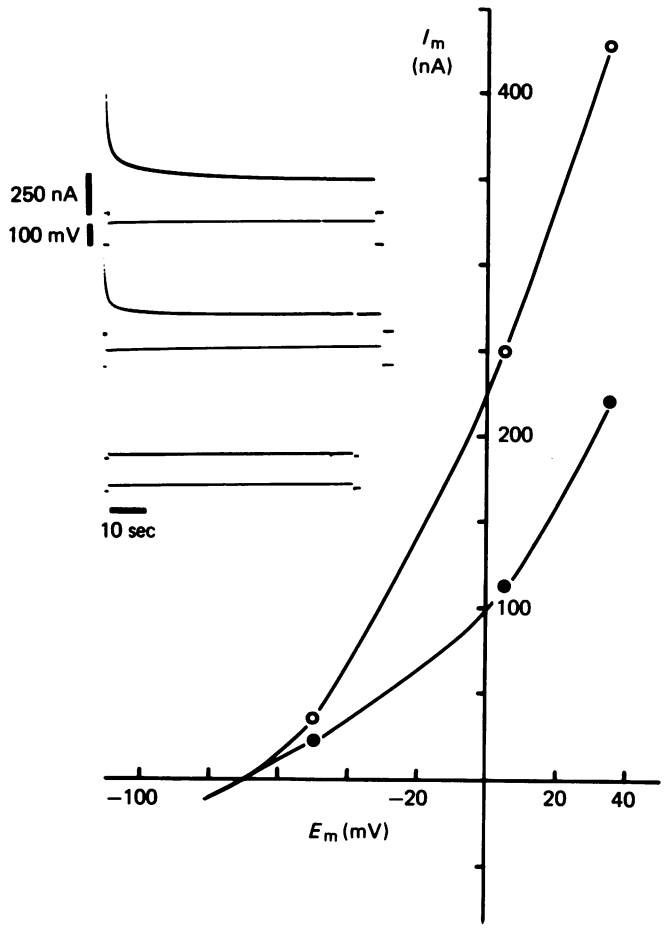


Fig. 3. Inset: voltage-clamp records showing outward current ($I_m$) during long step changes to different membrane potential levels. The rapid capacitative currents had decayed prior to full development of the peak outward current. Inward current associated with action potentials is not observable on these records due to the slow sweep velocity. Note that $I_m$ is essentially rectangular for a small step change of $E_m$. $I$–$V$ relations are shown at 1 (○) and 60 (●) sec after a step change in $E_m$.

The steady-state $I$–$V$ relation is plotted for the records shown in the inset. The filled symbols represent data obtained *before* stretch and the open data points represent the peak $E_m$ *during* stretch. At the resting potential, stretch produced a depolarization from −65 to −40 mV. This potential difference was reduced as the membrane potential was shifted to more positive values by passing current across the membrane. At +13 mV, no potential change was observed during stretch (reversal potential); from +13 to +40 mV, $E_m$ became less depolarized during application of stretch, i.e.

the sign of the stretch-induced potential changed sign. At the reversal potential the slope of the steady-state $I$–$V$ relation was 0·9 $\mu$mho and increased to 1·25 $\mu$mho during stretch. This represents a 40 % increase in membrane conductance during stretch. The input resistance of this cell estimated from the voltage change produced by an inward current step of 10 nA was 4·2 MΩ.

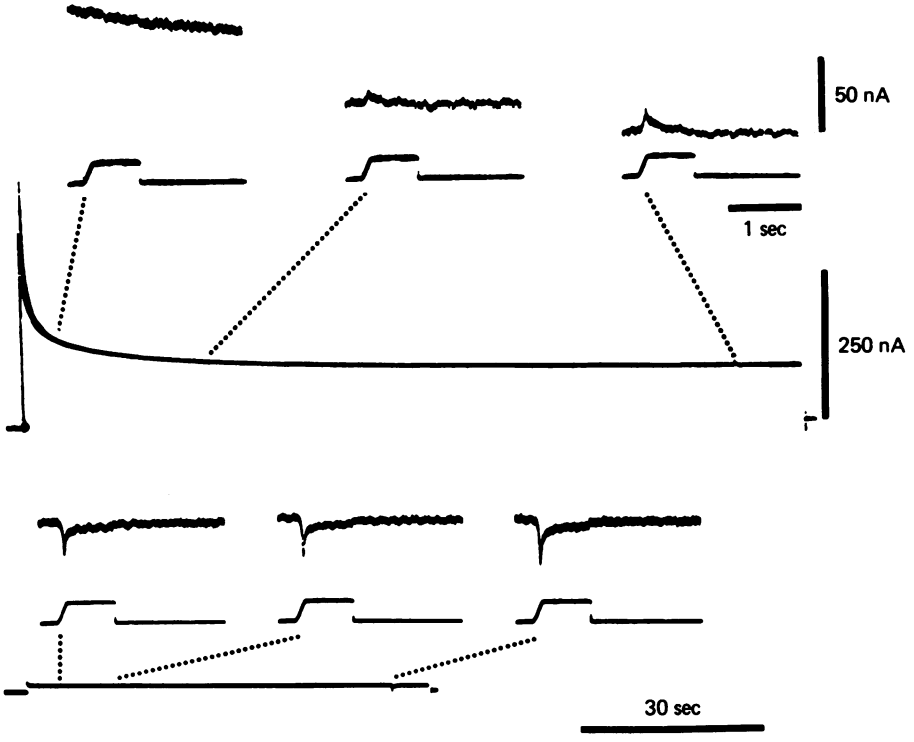


Fig. 4. Dependence of stretch-induced current on time after a step change in membrane potential.

Top record: envelope of outward current during changes of $E_m$ from the resting level (−70 mV) to +35 mV. Stretch was applied at different times after a change in $E_m$ as shown in the insets. Maximum current was obtained after steady-state outward current was obtained.

Bottom record: same procedure as above except $E_m$ shifted to −50 mV from −70 mV. Current calibration applied to both sets of records.

*Voltage clamp*

*Passive current inactivation.* It was observed previously that large positive potential shifts of the stretch receptor membrane produce a large outward current ($I_p$) that slowly inactivates with time (Nakajima & Onodera, 1969; Klie & Wellhöner, 1973). Fig. 3 shows this phenomenon and Fig. 4 shows that the stretch-induced current is smallest when $I_p$ is the greatest.

The inset in Fig. 3 shows three pairs of voltage clamp records obtained at different membrane potential levels. The top trace of each pair is membrane current associated with the potential change shown in the bottom trace. In the bottom pair, a rectangular change of membrane potential produced an approximately rectangular change of

membrane current when $E_m$ was shifted from the resting potential ($-70$ mV) to $-50$ mV. However, when the membrane potential was shifted to $+5$ from the $E_r$, there was an initial large positive outward current followed by a slow decline to a steady-state value. The top pair of records shows this clearly when the membrane potential was shifted from $E_r$ to $+35$ mV. In this case, the decline of the peak outward current to the steady-state level required more than 60 sec. Data from these records are plotted at the right 1 sec (○) and 60 sec (●) after the change in $E_m$. As the $E_m$ was shifted to more positive values, the $I_p$ obtained at 1 sec was almost twice as great as it was 60 sec later.

*Stretch-induced current*

*Relation between stretch-induced current and passive* $I_m$. It was found that the amplitude of the stretch-induced current (where the current $= I_m$ during stretch $- I_p$ without stretch) was related to the amount of passive membrane current during a step change of the membrane potential and the time after application of the voltage pulse as illustrated in Fig. 4. In the top set of records, $E_m$ was shifted from $-70$ to $+35$ mV; $+35$ mV was ascertained beforehand to be more positive than the reversal potential of the stretch-induced current. This potential change produced the typical large initial outward change in membrane current followed by a slow decline to a steady level. Stretch was applied in three consecutive runs, 5, 30 and 120 sec after the onset of the change in the membrane potential. The records are shown above the sustained record; these were obtained at higher amplification and sweep velocity. There was little or no detectable current 5 sec after the change of membrane potential, but 30 sec afterward a small outward current was observable and at 120 sec the outward current was more well developed. At still longer times the amplitude of the stretch-induced current was enhanced no further. The maximum current was obtained when $I_p$ produced by the potential shift was at a minimum. Since the minimum $I_p$ occurs sooner for smaller potential shifts, the fully developed stretch-induced current also occurs earlier. This could be demonstrated at a lower membrane level as shown in the bottom set of records in Fig. 4. Here, a $+20$ mV potential shift produced a brief transient which rapidly decayed to a steady state. In contrast, to the records shown in the top set of records, the stretch-induced current was almost as well developed 15 sec after the step-change in potential as it was 60 sec afterward. These results suggest that during a large increase in membrane conductance (presumably $G_K$) in response to a rapid potential change, there is suppression of the stretch-induced current or that $G_K$ does not allow its expression. An additional conductance change of an opposite sign that masks the current is another possibility. These alternatives will be discussed subsequently.

*I–V relations.* The exact membrane potential for reversal of the stretch-induced current was difficult to establish shortly after a shift in $E_m$ for reasons shown in Fig. 4. The stretch-induced current was largely obscured at positive membrane potential values for times as long as 1 min after a change in the membrane potential. By adopting the following procedure the inward current was enhanced and reliable $I–V$ relations could be obtained. The membrane potential was held to approximately $+40$ to $+50$ mV until inactivation of the large outward current was obtained. The $I_p$ was then shifted to a lower value (usually $-10$ mV) and stretch was

again applied, etc. This yielded reproducible 0-current values for the stretch-induced current and produced little undesirable effects such as changes in the resting potential or in the after-potential following stretch at the resting potential. The inset in Fig. 5 shows voltage clamp records of the stretch-induced current obtained in this way. The initial part of each trace represents the amount of $I_p$ necessary to hold $E_m$ to the value indicated at the right. At the more positive membrane potential values, stretch elicited an outward current consisting of a peak and steady phases;

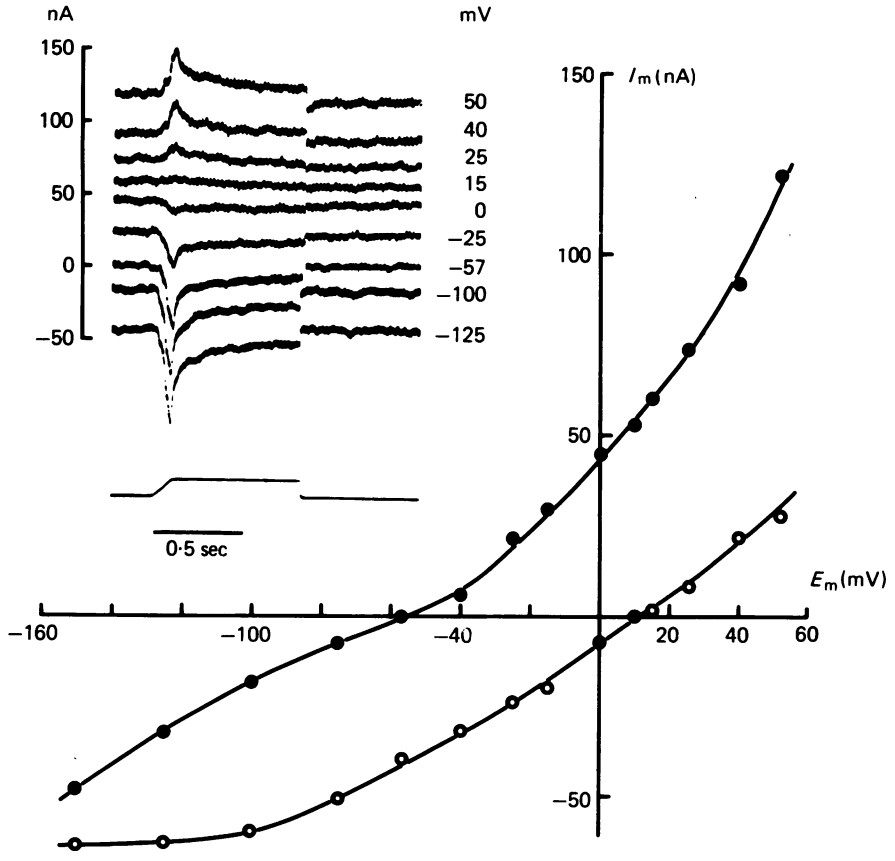


Fig. 5. Inset: voltage-clamp records of stretch-induced current obtained at the membrane potential levels indicated on the right. The steady-state level of membrane current is indicated by the offset of each record from the zero-current level.

*I–V* relations of the steady-state passive current (●) due to changes of membrane potential and the peak stretch-induced current obtained by subtracting the $I_p$ from the total membrane current during stretch.

this current was diminished as the membrane potential was reduced; a null-current was reached for both phases at the same $E_m$. As the membrane potential was further reduced, an inward stretch-induced current was recorded which increased in amplitude as the membrane potential became more negative. These data were obtained from the same cell shown in Fig. 2 and it can be seen that the reversal potential was identical with either method. The *I–V* curve plotted from the current records is illustrated in the graph in Fig. 5.

The passive steady-state relation before stretch is represented by filled circles and the active stretch-induced current is indicated by open circles. The slope conductance for the passive $I$–$V$ relation increased as the membrane was depolarized above $-40$ mV but remained quite constant from approximately $-40$ to $-100$ mV. At membrane potential levels more negative than $-100$ mV, membrane conductance again increased. The $I$–$V$ relation for the active phase of membrane current, i.e. the stretch-induced current, was clearly non-linear. The slope conductance approaches zero at values of $E_m$ more negative than $-100$ mV but increases as the membrane is depolarized. The slope conductance of the relation representing the stretch-induced current is about 0·7 $\mu$mho which represents about a 70% increase in the membrane conductance due to stretch compared to the membrane conductance measured from the steady-state passive $I$–$V$ relation at the reversal potential of the current (1 $\mu$mho). The average level of the reversal potential obtained from twenty-six cells in this way was $+13 \pm 6{\cdot}5$ mV (S.D.). The range was from $+3$ to $+30$ mV. In many preparations, it was possible to identify particularly long and short main dendrites. Invariably, those cells with long main dendrites had more positive reversal potentials than those with the short main dendrites. This suggests that most of the cell tc cell variability in the reversal potential can be attributed to the cable properties of the dendrites; the variability did not seem to be related to the input resistance of the membrane or the resting membrane potential.

*Effect of $Na^+$ substitutes*

*$I$–$V$ relations.* It has been reported in studies on different types of receptors (cf. Diamond, Gray & Inman, 1958; Ottoson, 1964; Brown *et al.* 1970) that a substantial fraction of the receptor potential remains in $Na^+$ substituted solutions and that more remains in Tris substituted $Na^+$ solutions than in choline (Obara, 1968) or arginine salines (Klie & Wellhöner, 1973). A systematic study of two of these $Na^+$ substitutes was made to evaluate the effect of these cations on the stretch-induced current and reversal potential.

Fig. 6*A* (filled circles) shows the $I$–$V$ relation of the passive membrane during changes in the membrane potential by the voltage clamp. The membrane potential was shifted initially to $+40$ mV and thereafter reduced in steps to the values shown in the diagram. The stretch-induced current in normal saline was obtained at each value of $E_m$ and is represented by the open circles. The current at $E_r$ was approximately $-25$ nA in the normal saline and showed the characteristic decline as the membrane potential was depolarized. At $+10$ mV the current reversed sign and at more positive potential values, it was outward or positive. Replacement of $Na^+$ with Tris produced a 5 mV reduction of the resting membrane potential and substantially reduced the receptor potential as shown in the inset. The current was reduced substantially but was still appreciable in the Tris-substituted saline. Stretch-induced current at $E_r$ was reduced to 5 nA, i.e. 20% remained in this solution. This reduction in the inward current was associated with a decrease in the 0-current potential from $+10$ to $-10$ mV. The outward current elicited by stretch at $+40$ mV was also reduced in the Tris saline to about 50% of the value in the normal saline. The solid squares indicate that there was also a small decrease in the passive membrane conductance in this saline but the change shown in this cell was not a constant

feature of all experiments in Tris. In many cells studied, there was a tendency for the passive membrane conductance to decrease somewhat during the experiment. This occurred even though there were no apparent changes in the input resistance of the membrane evaluated by a $-10$ nA current pulse applied at the resting membrane potential.

Fig. 6*B* shows the effects of $Na^+$ substitution with arginine. This cell was selected for illustration because it had a passive current voltage relation in the normal saline comparable to the cell in Fig. 6*A*. Replacement of $Na^+$ with arginine had virtually

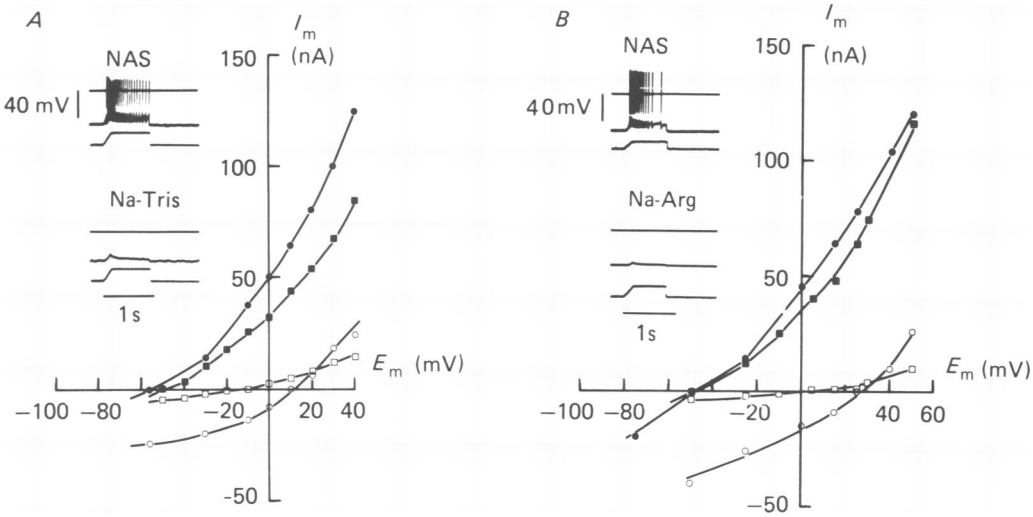


Fig. 6. Change in *I–V* relations of stretch receptor neurone in $Na^+$-substituted salines. *A*: Tris saline. *B*: arginine saline. Two different cells.

Filled circles and squares represent the steady-state *I–V* relation before stretch in normal saline (NAS) and Na-substituted saline respectively. The open circles and squares represent the peak stretch-induced current in normal and Na-substituted salines.

no effect on the resting membrane potential but slightly reduced the passive membrane current in the range $-20$ to $+30$ mV; thereafter, the membrane slope conductance was virtually the same in this saline as it was in normal saline. The stretch-induced current (open circles) was reduced more in this saline than it was in the Tris saline, i.e. the current at the resting potential in arginine saline was only 10 % of the value in normal saline. This was manifested as a small receptor potential as shown in the inset. The reversal potential shifted significantly as the $Na^+$ was replaced with arginine. In normal saline the reversal potential was about $+25$ mV and in the arginine saline it was reduced to about $-2$ mV for a total change of $-27$ mV.

*Dependence of stretch-induced current on $Na^+$ concentration.* The inward current was evaluated in three different cells at different $Na^+$ concentrations as Tris replaced $Na^+$ in the external medium. The cells were exposed to normal saline after each exposure to a $Na^+$-substituted saline. The results were normalized by assigning the inward current at the resting potential in normal saline a value of $-1{\cdot}0$. Values of the stretch-induced current at other $Na^+$ concentrations were expressed as the ratio

of this value. In Fig. 7*A*, which shows Tris substitution of $Na^+$, the inward current at $E_r$ is seen to vary linearly with the $Na^+$ concentration in the external medium. The final value of the current in 2 mM-Na-Tris saline still represents a significant fraction of the current measured in normal $Na^+$. In the cell represented by filled circles, 25% of the current remained even though $Na^+$ had been reduced tenfold from 210 to 21 mM. In the cells represented by open circles and squares, the current was reduced to 35 and 50% of that in normal saline for a reduction in $Na^+$ from 210 to 2·1 mM.

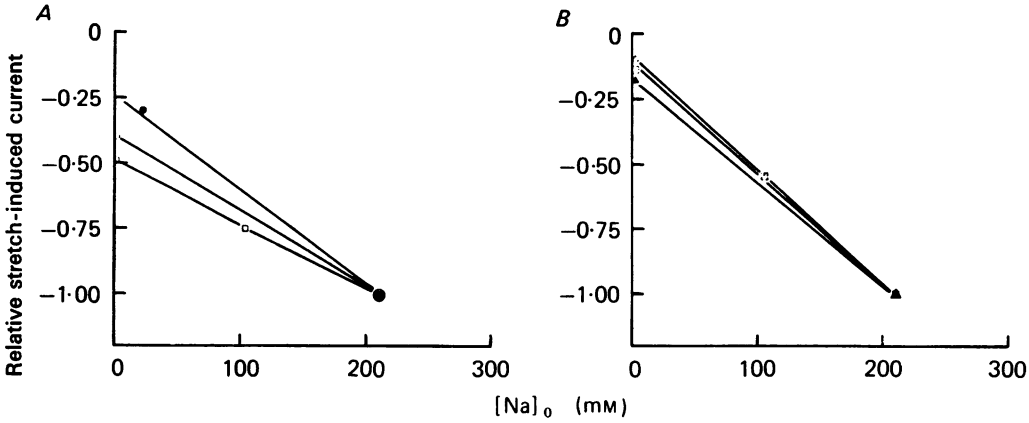


Fig. 7. Relationships between peak stretch-induced current and Na concentration. *A*: peak current in Tris-Na solutions. *B*: peak current in arginine-Na solutions. Peak current measured at a holding potential which corresponded to the resting potential of the cell; each symbol represents a different cell. The peak current in each test saline is expressed compared with that in normal saline (210 mM-$Na^+$); latter was assigned a value of −1·0.

Data obtained in arginine (Fig. 7*B*) also indicated a linear dependence of the stretch-induced current on the external $Na^+$ concentration; however, arginine appeared less permeable than Tris as indicated by the greater reduction in the inward current as $Na^+$ was systematically replaced by arginine. There was also less cell-to-cell variation. Inward membrane current in 2·1 mM-Na arginine solution represented only 10–18% of the stretch-induced current measured in the normal saline. These data compare favourably with changes in the reversal potential (Fig. 8) which indicates that the permeability ratio of arginine/$Na^+$ is less than for Tris/$Na^+$.

*$Na^+$ permeability ratios.* By systematically changing the amount of $Na^+$ in the external medium and observing the changes in the reversal potential of the stretch-induced current, estimates of the permeability ratios of the ion substitutes to $Na^+$ were obtained. In these experiments the cell was routinely returned to the normal saline between the test salines. If repeated determinations of the reversal potential were made in a given $Na^+$ concentration, the results were averaged for purposes of the data analysis.

Permeability ratios were obtained from the relation (Brown & Saunders, 1977):

$$P_{Na}/P_X = \frac{a}{bm + a} \qquad (2)$$

where $a$ and $b$ represent the intercept and slope of the relation, exp $E_m F/RT$ *vs.* concentration of $Na^+$ in the external solution as $Na^+$ is replaced by a substitute cation. A value of 25 was used for $F/RT$ and $m$ is the total cation concentration. Plots of this relation for two different cells in Tris-$Na^+$ salines are shown in Fig. 8*A*. The line connecting the points was drawn by eye. From the slope and intercept a value of $P_{Tris}:P_{Na}$ of 0·31 was obtained. This indicates that as large a cation as Tris (mol. wt. = 121), has a very significant permeability in the membrane during stretch.

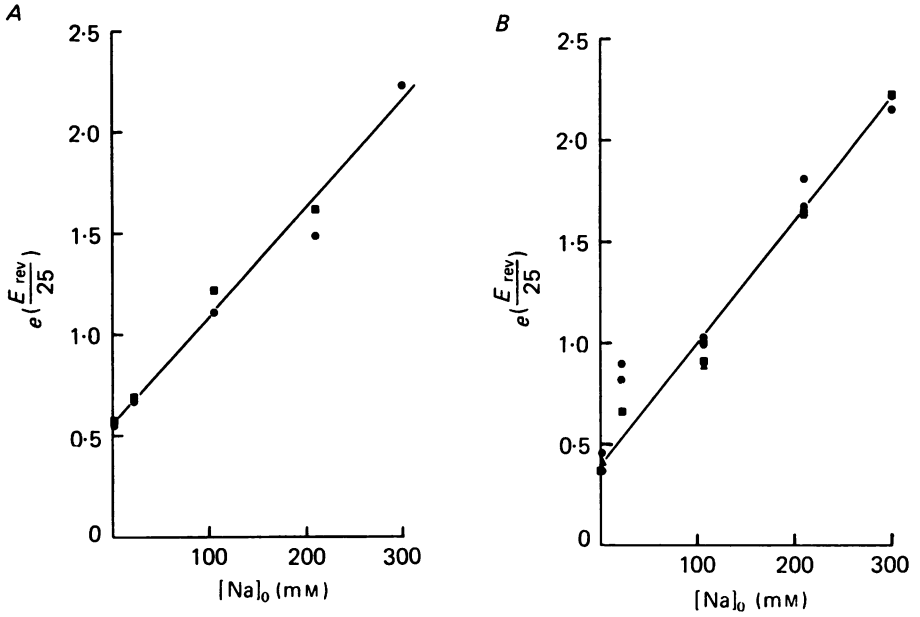


Fig. 8. Tris-Na and arginine-Na permeability ratios in stretch receptor. *A*: relation between exp (reversal potential/25) and Na concentration in Tris-Na solutions for three different cells denoted by different symbols, $P_{Tris}/P_{Na}$ = 0·31. *B*: same as *A* except arginine-Na solutions for four cells, $P_{arg}/P_{Na}$ = 0·26.

Arginine appears to be somewhat less permeable cation than Tris judging from a similar analysis of four cells shown in the plot of Fig. 8*B*. In this case, the line fit by eye falls quite close to all of the transformed data points except those at the 21 mM-$Na^+$ concentration. The reason for this is not clear but in practice this represents a small change in the reversal potential of the stretch-induced current between arginine solutions containing 105 mM-$Na^+$ and those containing 21 mM-$Na^+$ (average change of the reversal potential in these two solutions = 5 mV). The value of $P_{Arg}:P_{Na}$ obtained from the relation in Fig. 8*B* was 0·24 indicating that $Na^+$ is only about 4 times more permeable than the much larger amino acid molecule.

*Effect of* $Ca^{2+}$. The preparation tolerated low $Ca^{2+}$ solutions very well, provided that the time for exposure was relatively short and the cell was returned to normal saline between the test salines. Results from a voltage-clamp experiment on one cell as $Mg^{2+}$ replaced $Ca^{2+}$ in the external saline are shown in Fig. 9. The $I$–$V$ relations were obtained after the preparation was exposed for 15 and 20 min in the 0·135 and 1·35 mM-$Ca^{2+}$ salines respectively. Exposure to low $Ca^{2+}$ salines produced a syste-

matic reduction in the $E_r$ and the slope conductance of the membrane was generally increased. Reducing $Ca^{2+}$ also had systematic effects on the stretch-induced current. The inset shows the current obtained at $-60$ mV in reduced $Ca^{2+}$ salines. It was increased twofold for a tenfold reduction in $Ca^{2+}$ and increased threefold for a hundredfold reduction in $Ca^{2+}$ concentration. This is reflected in the $I-V$ relation which shows that the slope conductance for the active phase is increased on the negative and positive side of the reversal potential. The membrane conductance at the 0-current potential of the stretch-induced current indicates an approximate doubling of the stretch-induced conductance change for each tenfold change in $Ca^{2+}$ concentration, i.e. the conductance increased from 0·25 $\mu$mho in normal saline to 0·66 and 1·5 $\mu$mho in the 1·35 and 0·135 mM-$Ca^{2+}$ salines, respectively.

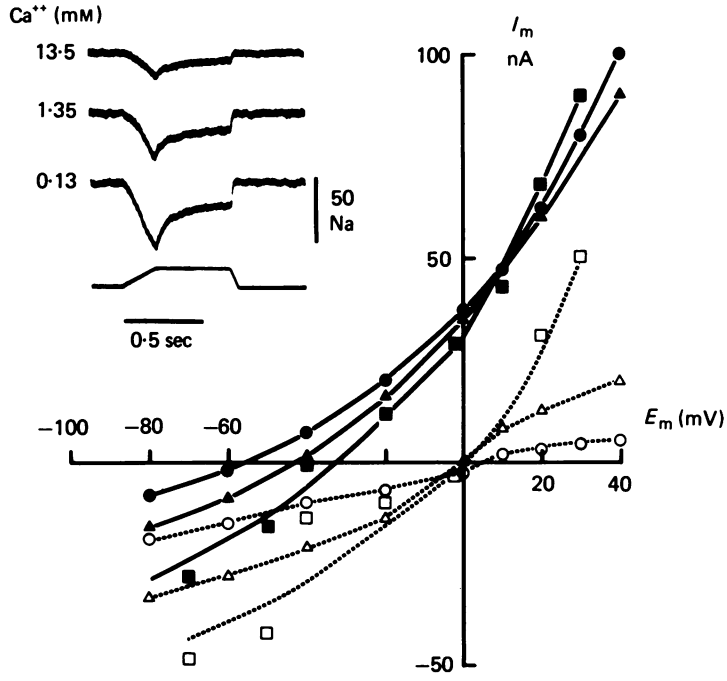


Fig. 9. $I-V$ relations in different $Ca^{2+}$ concentrations. Filled symbols represent the steady-state passive relation and open symbols represent the peak stretch-induced current. Holding potential at $E_m$ in each test saline. Normal saline (○, ●); 1·35 mM-$Ca^{2+}$ (△, ▲); 0·13 mM-$Ca^{2+}$ (□, ■). Inset: traces of current in different $Ca^{2+}$ solutions at about resting membrane potential.

$Ca^{2+}$ was also reduced in a solution containing a relatively impermeant cation (Tris) to unmask a possible increase in $Ca^{2+}$ conductance during the active phase (Brown *et al.* 1970). The results of one experiment are shown in Fig. 10. By comparing the left and right panels, it is evident that a reduction of $Ca^{2+}$ in Tris saline produces a large increase of the stretch-induced current at membrane potential levels more positive and negative than the reversal potential; however, the potential at which the current's sign was reversed was little affected by the change in $Ca^{2+}$. The peak current values in these salines are shown in the $I-V$ relation. The open circles show

the voltage dependence of the current in normal saline. Current at the resting potential (−60 mV) was −25 nA and its sign was reversed at about +10 mV. Replacement of $Na^+$ with Tris produced a large reduction in the stretch-induced current to about 5 nA or 20% of the control value. There was also a shift in the reversal potential from +10 to −10 mV. Reduction of $Ca^{2+}$ produced a fourfold increase in current at −60 mV, which was almost equivalent to that in normal saline. There was essentially no change of the reversal potential upon reduction

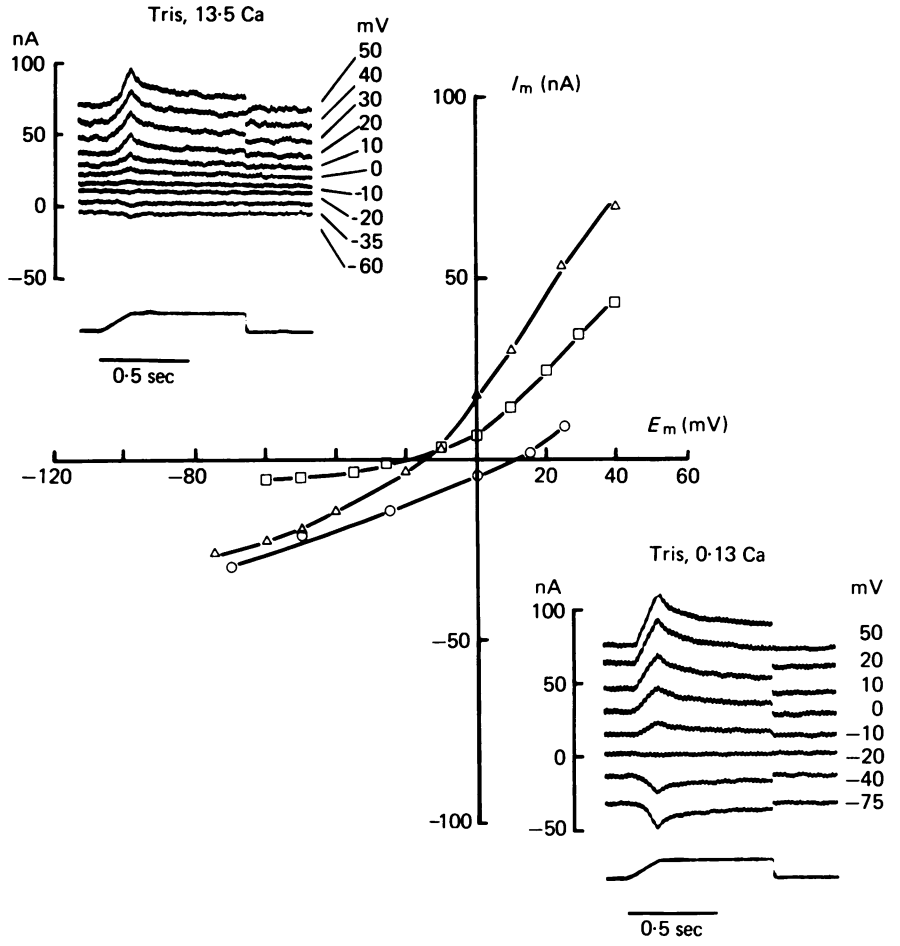


Fig. 10. Effect of reduced $Ca^{2+}$ on stretch-induced current in Tris substituted-Na saline.

Insets: traces of the current in Tris normal saline (top) and low $Ca^{2+}$ Tris saline (bottom). Membrane current required to sustain the membrane potential is represented by the offset of each current trace from the zero-current level. Voltage-clamped $E_m$ indicated on the right.

*I–V* curves: peak stretch-induced amount in normal saline (○), in saline with all $Na^+$ substituted with Tris (□), and in low $Ca^{2+}$ Tris saline (△).

of $Ca^{2+}$; if anything, a slight positive shift occurred. Thus, there appears to be no significant permeability increase to $Ca^{2+}$ during stretch even in Tris solutions. Rather, $Ca^{2+}$ seems to play a major role in moderating the monovalent cation permeability.

*Slow stretch-induced current*

It was observed during current clamp experiments that most cells had a slow depolarizing component during stretch that became more apparent as the membrane was systematically depolarized. This potential change had a slow time course and outlasted the stretch by 1–2 sec. This was in contrast to the behaviour of the stretch-induced potential change (see Fig. 2) which consisted of an initial peak and a later steady phase both of which declined as the cell was depolarized. Furthermore, the

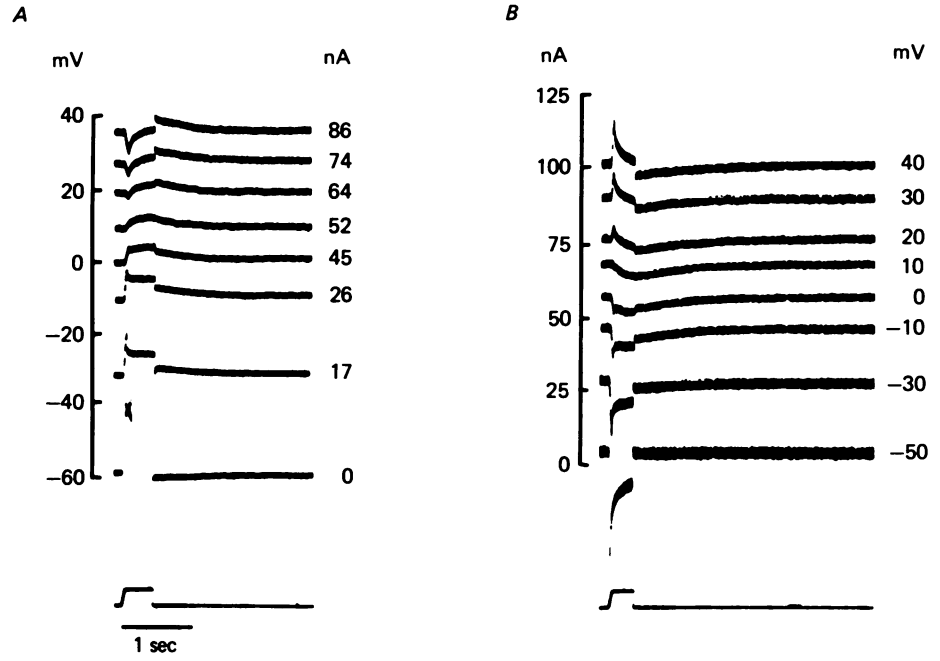


Fig. 11. Slow stretch-induced current. *A*: current clamp records showing a slow positive potential change that develops during stretch as the membrane is depolarized. The potential change is most obvious at the reversal potential of the fast stretch-induced potential change and appears as a positive after-potential at more negative levels of membrane potential. Currents to hold the membrane at the different levels indicated to the right. *B*: voltage clamp records of slow stretch-induced current and stretch-induced current at different levels of $E_m$ (right). The slowly developing slow component appears in isolation at the 0-current level of membrane potential for the usual stretch-induced current (+10 mV). Polarization indicated to the right.

slow component gave the appearance of a positive after-potential following stretch when the membrane was slightly depolarized from its resting level and the appearance of a negative after-potential when the membrane was in a hyperpolarized state. In many cells, the presence of this slow component of the receptor potential made determination of the reversal potential difficult because it was still evident when the usual stretch-induced receptor potential was effectively zero. However, it became apparent that this slow component appeared in its purest form at the reversal potential for the usual stretch-induced potential change.

Examples of this are shown in Fig. 11*A*. At the resting potential stretch elicits

a depolarizing receptor potential and a series of action potentials; cessation of stretch is followed by a slow negative after-potential. As the membrane is depolarized with constant current the after-potential following stretch is more positive than the pre-stretch level and slowly declines to the pre-stretch membrane potential level. At the reversal potential for the usual stretch-induced receptor potential, a slowly developing depolarization is observed that declines slowly following cessation

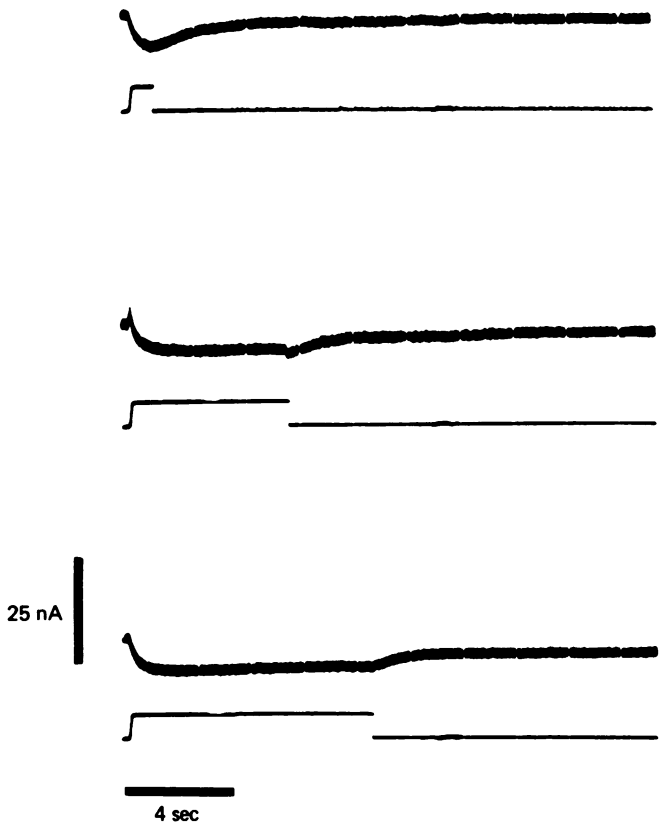


Fig. 12. Slow component of the current obtained with different durations of stretch near the reversal potential of the stretch-induced current. A slight decay of slow component can be observed with long stretches.

of stretch. This 'tail' increases in amplitude as the membrane is depolarized to higher levels as indicated by the potential jump at release of stretch. Records of membrane current from the same cell during voltage-clamp are shown in Fig. 11*B*. At $-50$ mV, stretch induces a large peak inward current that declines to a lower level as stretch is sustained. Release of stretch produces a small outward current which declines to the pre-existing level. As the membrane potential is shifted to more positive values, a slow 'tail' of inward current is evident following cessation of the stretch. At the zero-current membrane potential level for the usual stretch-induced current, a well developed slow inward current is seen to remain that requires approximately 2 sec to decline to the pre-stretch level. The magnitude of this current is augmented as the membrane is further depolarized.

By clamping the membrane potential to the reversal potential for the usual stretch-

induced current, the time course of the slow stretch-induced current was studied during changes of duration of stretch (Fig. 12). The top trace shows that the inward current develops a maximum approximately 1 sec after application of stretch. The decline of the membrane current to the pre-stretch level has a slower time course than the onset. The half-time for the former was 0·4 sec and the latter, 2 sec. For longer stretches (middle and bottom trace), a small decline from the peak was observed about 1 sec after the stretch was initiated. This was followed by the usual slow decline after stretch was released. As shown in the bottom trace in Fig. 12, the inward current remains for stretches of up to 10 sec.

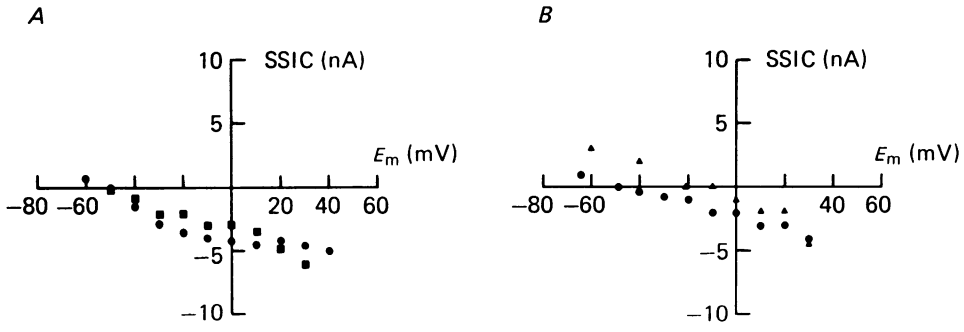


Fig. 13. *I–V* relations of slow stretch-induced current in different salines. A: filled circles illustrate the slow portion in normal saline; squares show *I–V* relation of slow portion in K-free saline. *B*: *I–V* relations of slow stretch-induced current in normal saline (filled circles) and in K-free 0·1 mM-$Ca^{2+}$ saline (filled triangles). In the latter saline the resting potential was reduced to −20 mV after an extended exposure. Different cell from that in *A*.

*Ion substitutes and I–V relations of the slow stretch-induced current.* The filled circles in Fig. 13*A* show the *I–V* relation for the slow part of the current in normal saline from a voltage-clamped cell. Since the maximum was obscured by the stretch-induced current at all membrane potential levels other than its reversal potential, the tail current at release of 1 sec stretches was measured. This was considered to give a good approximation of the maximum slow component (see Fig. 12). The data obtained indicate that the slow stretch-induced current increases linearly as the membrane is depolarized to approximately zero membrane potential. The increase is somewhat less for more positive membrane potential values. There was a clear reversal of the slow current phase at −55 mV in this cell. The slope of the *I–V* relation indicates that this current is produced by a conductance decrease to a positive ion species with an effective e.m.f. close to or somewhat more positive than the resting potential of the cell or alternatively a corresponding change to an outward-going anion species.

Since a decreased $K^+$-conductance during stretch could account for these results, the slow stretch-induced current was investigated by exposing the cell to a $K^+$-free solution. As shown in Fig. 13*A* by the squares, the reversal potential was not appreciably affected by the $K^+$-free solution. Depolarizing the membrane in a $K^+$-free, Ca-free solution did produce a positive shift of the reversal potential of the slow portion of the current as shown by triangles in Fig. 13*B*.

*Intracellular $Cl^-$ and $K^+$ measurements*

An attempt was made to estimate the $Cl^-$ equilibrium potential in the stretch receptor by measuring intracellular $Cl^-$ activity ($a^i_{Cl}$) with $Cl^-$ liquid ion-exchange micro-electrodes and Ag/AgCl wire-in-glass electrodes as described in Methods. These electrodes were larger than the KCl electrodes (approx. 1 $\mu$m) and some difficulty was experienced in penetrating the cells with them. Six of these experiments were considered adequate (1) by the agreeement of the pre- and post-experimental calibration of the electrodes and (2) because little or no change in the resting potential was observed upon insertion and removal of the KCl electrode. The results are shown in Table 2. Cells 1 and 2 are repeated observations on the same cell with the same type

TABLE 2. Intracellular Cl activity

| Cell | Electrode | $a^i_{Cl}$ (mM) | $E_{Cl}$ (mV)* | $E_m$ (mV) |
|---|---|---|---|---|
| 1 | (CLIX)† | 14 | −62 | −70 |
| 2 | (CLIX) | 14 | −62 | −70 |
| 3 | (CLIX) | 18 | −56 | −67 |
| 4 | (CLIX) | 14 | −62 | −67 |
| 5 | (AgCl) | 16 | −59 | −70 |
| Mean (± S.D.) | | 15·2 ± 1·8 | −60·2 ± 2·7 | −69 ± 1·6 |

$$* E_{Cl} = 57 \log_{10} \frac{a^i_{Cl}}{174}.$$

† Chloride liquid ion-exchange.

TABLE 3. Intracellular K activity

| Cell | $a^i_K$ (mM) | $E_K$ (mV)* | $E_m$ (mV) |
|---|---|---|---|
| 1 | 94 | −78 | −55 |
| 2 | 102 | −80 | −64 |
| 3 | 160 | −91 | −64 |
| 4 | 169 | −93 | −67 |
| 5 | 140 | −88 | −72 |
| Mean (± S.D.) | 133 ± 34 | −86 ± 7 | −64 ± 6 |

$$* E_K = 57 \log_{10} \frac{4}{a^i_K}.$$

of ion-exchange electrode. An Ag/AgCl electrode was used in cell 5. The external $Cl^-$ was empirically determined from measurements with a Ag/AgCl electrode and found to be 174 mM (mean of several observations with several different electrodes). The mean $a^i_{Cl}$ from all five determinations yields an intracellular $a^i_{Cl}$ value of 15 mM and an $E_{Cl}$ of −60 mV. Since the mean resting potential in these cells was −69 mV, the $Cl^-$ equilibrium potential is more positive than $E_m$, i.e. there is more intracellular $Cl^-$ than would be anticipated from a passive distribution of $Cl^-$.

Intracellular $K^+$ activity ($a^i_K$) was measured in five cells and the results are shown in Table 3. The cells are ranked according to their resting potential. There was more variability in the resting potential of these cells than those studied with $Cl^-$ electrodes and this seemed to be reflected in the values of $a^i_K$ to some extent.

Cell 1 with the lowest $E_m$ (−55 mV) also had the lowest $a_K^i$ (94 mM); cells with more negative resting potentials tended to have higher $a_K^i$s. The mean value of $a_K^i$ in the five cells studied was 133 mM which corresponded to an average $E_K$ of −86 mV. This is more than 20 mV more negative than the resting potential of the cells as a group.

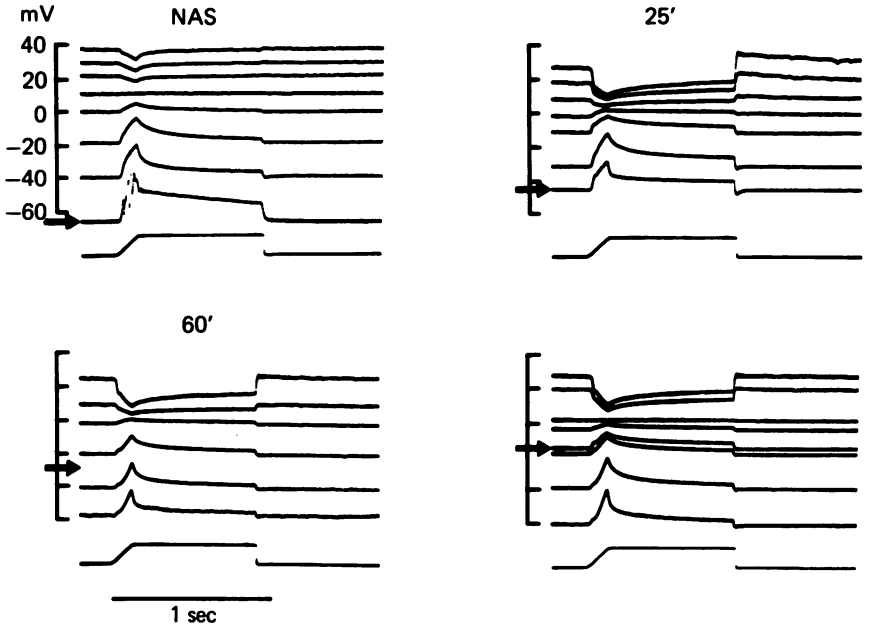


Fig. 14. Membrane potential changes during stretch at different $E_m$ following the substitution of K-free, 0·1 mM-$Ca^{2+}$ saline. The current-clamped membrane potential levels are indicated on the left and the arrow indicates the resting membrane potential level at the specified time in the experimental saline.

*Changes of $a_K^i$ and receptor potential.* It has been found in voltage-clamp experiments that removal of potassium causes a reduction of the light-induced current of the photoreceptor in *Balanus* and that reduction of $Ca^{2+}$ in $K^+$-free solution reverses the effect (Brown & Ottoson, 1976). It was of interest to examine whether or not a similar effect occurs in the stretch receptor neurone. Fig. 14 shows four panels of current clamp records obtained in $K^+$-free, low $Ca^{2+}$ salines at the times indicated above each panel. A 25 min exposure produced a reduction of $E_m$ from −60 to −45 mV and a shift of the reversal potential from +10 to approximately +5 mV. At 60 and 80 min, there was no change in the reversal potential, but the resting potential continued to decline until at 80 min it was only −13 mV. Although the receptor potential was small at this membrane potential, it could be almost restored to the control amplitude by hyperpolarization of the membrane before stretch was applied.

A dramatic reduction in the $a_K^i$ occurs upon exposure of the receptor to a $K^+$-free solution as shown in Fig. 15, which shows results of a cell studied with a $K^+$ ion-exchange micro-electrode. This cell had an $E_r$ of −67 mV at the time $K^+$-free solution was introduced into the bath. There was an initial hyperpolarization of the membrane

to −90 mV 15 min after $K^+$-free and this was followed by a slow steady decline of $E_r$ for the remainder of an hour. The $a_K^i$ showed a monotonic decrease of $a_K^i$ at the rate of about 2·5 m-mole/min over this same time. After 60 min, the $a_K^i$ had dropped to only 20 mM and the $E_r$ was −40 mV. However, as shown in Fig. 14, a well developed receptor potential can still be elicited under these conditions.

Restoration of the $K^+$ to the bath restores the $a_K^i$ to the original value in approximately 45 min; the $E_r$ was slightly more negative than the control value at this time. Reducing the $Ca^{2+}$ one hundredfold during an exposure to $K^+$-free accelerates the rate of $K^+$ loss as shown at 120 min; however, reduced $Ca^{2+}$ did not appear to augment a loss of $K^+$ if applied concomitant with the reduction in $K^+$ (160 min).

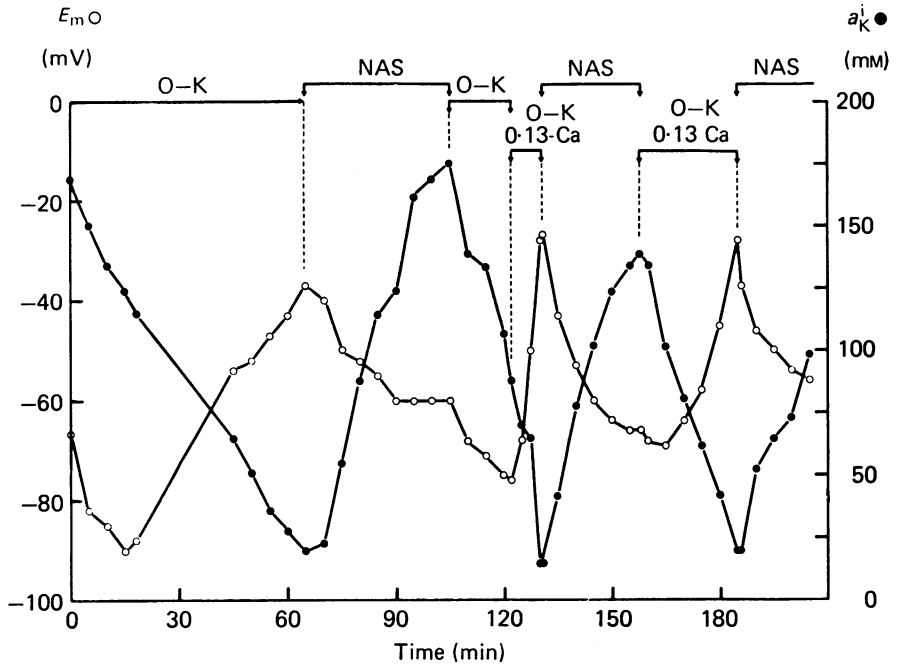


Fig. 15. Effect of K-free and K-free-0·13 $Ca^{2+}$ solutions on intracellular K-activity measured with a K-sensitive liquid ion exchanger micro-electrode. Open circles represent measurements of the resting membrane potential (left ordinate) and filled circles represent $a_K^i$ (right ordinate). The changes of solutions are shown at the top.

## DISCUSSION

Most of the present knowledge about ionic currents involved in receptor functions derive from voltage clamp studies on photoreceptors. Corresponding studies on mechanoreceptors have been difficult for various reasons. The main reason is that there are few mechanoreceptors which are large enough to allow multiple electrode impalement. Another reason lies in the difficulty of preventing the intracellular electrodes used for recording and passing current from being dislodged during application of mechanical stimulation.

In the present study, we used a technique which allows stretching the receptor without causing an appreciable displacement of the cell body of the neuron: it is mainly the dendrites which are stretched. As a consequence, it was possible to con-

tinually record from the neurons with repeated application of stretch for 6–8 hr without dislodging the electrodes. This technique enabled a systematic analysis of the ionic currents underlying the receptor potential of the stretch receptor. The results, as far as the reversal potential for the stretch-induced current are concerned, are in general agreement with the values obtained by Klie & Wellhöner (1973) who also used the voltage clamp technique. They obtained satisfactory results from forty of 800 stretch receptor preparations and they found that the reversal potential of the stretch-induced current for most cells was about +25 mV but sometimes as low as +5 mV. We obtained a mean value for the reversal potential of +13 mV for all cells in our study; values as high as +30 mV and as low as +3 mV were obtained.

These values differ greatly from those reported earlier in the literature. Thus, in 1962, Terzuolo & Washizu, utilizing an indirect method for determining the reversal potential, obtained a value of 0 mV. Obara (1968) reported reversal potentials of −20 to −30 mV. In both of these investigations, the reversal potential was obtained from extrapolation of a partial $I$–$V$ curve.

There appear to be several reasons why different investigations obtained different values. Microscopic observation of the cells suggests that the variability might be related to the cable properties of the dendrites since it was observed that cells with long main dendrites invariably had the most positive reversal potentials. Part of the variability also lies in the method used for measurement of the sign-reversal of the stretch-induced current. Since the current is diminished for several seconds after the depolarization of the membrane, it is readily measured only after $I_p$ has reached a steady-state value. This may indicate some interaction between the current and $I_p$ or it may simply indicate that the receptor site is inadequately clamped when the $I_p$ is high, i.e. in the region of outward rectification. In this regard, it should be stressed that the relations between the current and $E_m$ in the present study were obtained when $I_p$ was in the steady state, and, as far as we could determine. The relation obtained before a steady-state $I_p$ yielded essentially the same reversal potential. However, if it is assumed that space-clamping is a problem in these cells, then the cells with the shortest dendrites and less positive reversal potential should provide the closest estimate of the 'true' value of the reversal potential. For the above reasons, the earlier work on this preparation which extrapolated partial $I$–$V$ curves to estimate the reversal potential may provide quite accurate values of the 'true' reversal potential, even though the non-linear character of the stretch-induced current-$E_m$ relation was not taken into account.

Data from the present study indicate that the stretch receptor is not very selective to different cations of widely varying size, i.e. large cations such as Tris and arginine are as much as one third to one quarter as permeable as the much smaller unhydrated $Na^+$ ion. Several other studies have reported a receptor potential of significant amplitude in media containing $Na^+$ substitutes (Edwards, Terzuolo & Washizu, 1963; Obara, 1968; Klie & Wellhöner, 1973), but estimates of selectivity were not obtained. This poor cation selectivity accounts for the fact that the changes in the 0-current potential show less than an ideal change when $Na^+$ is replaced by a seemingly impermeant cation. It is worthy of note that replacing $Na^+$ with arginine in hypertonic solutions (500 mM) with a normal complement of divalent cations produced a 45 mV change in the reversal potential per decade change in $Na^+$ concentration over

the range 105–500 mM-$Na^+$. This makes it clear that the membrane can behave as an approximate $Na^+$ electrode under certain experimental conditions.

$Ca^{2+}$ does not appear to participate directly in the stretch-induced current as evidenced by the lack of reversal potential changes in $Ca^{2+}$ salines of different concentration, whether the $Ca^{2+}$ changes were made in normal $Na^+$ or $Na^+$-substituted salines. However, $Ca^{2+}$ does affect the stretch-induced current by suppressing the normal monovalent cation current and as shown in Figs. 9 and 10, it can suppress a Tris current as well as a $Na^+$ current. A reduction of $Ca^{2+}$ can also increase the net efflux of $K^+$ when the stretch receptor is exposed to $K^+$-free solutions as demonstrated with the $K^+$ liquid ion exchanger electrodes.

The experiments conducted with the $Cl^-$ and $K^+$-sensitive micro-electrodes are relevant to the mechanism of the slow stretch-induced current and generation of the i.p.s.p. in this preparation. Intracellular $Cl^-$ ($a^i_{Cl}$) has been measured in crayfish axons with both Ag/AgCl electrodes (Strickholm & Wallin, 1975) and with ion exchanger electrodes (Cornwall, Peterson, Kunze, Walker & Brown, 1970). The latter estimate (13·7 mM) was lower than the former (25·2 mM) but both were in qualitative agreement that $E_{Cl}$ was more positive than $E_m$. We found no difference between estimates of $a^i_{Cl}$ depending on electrode type in the stretch receptor and the $a^i_{Cl}$ we obtained (about 15 mM) is very close to the values Cornwall *et al.* obtained in axon. There remains the possibility that our estimate of $a^i_{Cl}$ is too high since there may have been some leakage from the KCl electrodes used for measurement of $E_m$. However, control experiments with similar electrodes in a different preparation produced results that were inconsistent with any significant leakage from KCl electrodes under the same conditions (Brown, 1976). Thus, $E_{Cl}$ in crayfish stretch receptor and axon appears to be more positive than $E_m$; in both preparations, $Cl^-$ is not in a Donnan equilibrium. It has been demonstrated that the i.p.s.p. in crayfish stretch receptor is dependent upon both $K^+$ (Edwards & Hagiwara, 1959) and $Cl^-$ (Hagiwara, *et al.*, 1960) conductance changes. Our results from the $K^+$ and $Cl^-$ electrodes support this notion, since $E_{Cl}$ appears to be too near $E_m$ to account for the generally negative-going i.p.s.p. One consequence of this proximity of $E_{Cl}$ and $E_m$ would be that the sign of the i.p.s.p. would be dependent on $E_m$ (Kuffler & Eyzaguirre, 1955) and that the large negative i.p.s.p.s that seemed independent of $E_m$ reported by Meyer & Lux (1974) could be due to a predominant $K^+$ component. It should be noted that our value for $E_K$ based on the ion-exchanger electrode ($-86$ mV) is considerably more negative than a previous estimate ($-70$ mV) obtained with less direct techniques (Ozawa & Tsuda, 1973).

The slow stretch-induced current identified and described in the present study was a demonstrably inward current at $E_m$ more positive than $E_r$ and an outward current at $E_m$ more negative than $E_r$. It is tentatively identified as predominantly a $Cl^-$ current for two reasons: (1) the similarity of the reversal potential and $E_{Cl}$ measured with ion sensitive electrodes and (2) that changes in the reversal potential did not follow the $K^+$ equilibrium potential but were in the anticipated direction of the $Cl^-$ equilibrium potential. Thus, when both external K and Ca were removed from the saline, the membrane was depolarized and the reversal potential shift was in the same direction. $Cl^-$ likely moves into the cell under these experimental conditions which would result in a more positive $E_{Cl}$.

The slow stretch-induced current has the feature that it increases with $E_m$ and consequently is more apparent as the membrane is depolarized and the stretch-induced current is reduced. Thus, at intermediate membrane potentials between the resting potential and the reversal potential, the total stretch-induced current is composed of both components.

It is concluded from these observations that the receptor potential can be represented by at least three components of membrane current: (1) stretch-induced current, (2) the slow component of this and (3) $I_p$. The first component can be isolated in a relatively pure form at the resting potential and $Na^+$ is the indicated current carrier. The second component can be isolated at the 0-current potential of the stretch-induced current and $Cl^-$ is the suggested current carrier. $I_p$, a presumptive $K^+$ component may interact with the stretch-induced current or alternatively may not allow expression of this current in voltage clamp experiments, especially when $I_p$ is large, i.e. at high positive membrane potentials soon after a clamp pulse.

The authors wish to express their gratitude to Toni Gillett and Bo Johanson for excellent technical assistance. This work was supported by a grant from the Swedish Medical Research Council (B77-14X-00043-13B and B78-14X-00043-14C) and by a grant from the N.E.I. of the N.I.H. (EY 00762).

## REFERENCES

BROWN, H. MACK (1976). Intracellular $Na^+$, $K^+$ and $Cl^-$ activities in large barnacle photoreceptors. *J. gen. Physiol.* **68**, 281–296.

BROWN, H. MACK, HAGIWARA, S., KOIKE, H. & MEECH, R. (1970). Membrane properties of a barnacle photoreceptor examined by the voltage-clamp technique. *J. Physiol.* **208**, 385–413.

BROWN, H. MACK & OTTOSON, DAVID (1976). Dual role for potassium in *Balanus* photoreceptor: antagonist of calcium and suppression of light-induced current. *J. Physiol.* **257**, 355–387.

BROWN, H. MACK & SAUNDERS, JAMES H. (1977). Cation and anion sequences in dark-adapted *Balanus* photoreceptor. *J. gen. Physiol.* **70**, 531–543.

BROWN, J. E. & MOTE, M. I. (1974). Ionic dependence of reversal voltage of the light response in *Limulus* ventral photoreceptor. *J. gen. Physiol.* **63**, 337–350.

CORNWALL, M. C., PETERSON, D. F., KUNZE, D. L., WALKER, J. L. & BROWN, A. M. (1970). Intracellular potassium and chloride activities measured with liquid ion exchanger microelectrodes. *Brain Res.* **23**, 433–436.

DIAMOND, J., GRAY, J. A. B. & INMAN, D. R. (1958). The relation between receptor potentials and the concentration of sodium ions. *J. Physiol.* **142**, 382.

EDWARDS, C. & HAGIWARA, S. (1959). Potassium ions and the inhibitory process in the crayfish stretch receptor. *J. gen. Physiol.* **43**, 315–321.

EDWARDS, C., TERZUOLO, C. & WASHIZU, Y. (1963). Effect of changes of ionic environment upon an isolated crustacean sensory neuron. *J. Neurophysiol.* **26**, 948–957.

HAGIWARA, S., KUSANO, K. & SAITO, S. (1960). Membrane changes in crayfish stretch receptor neuron during synaptic inhibition and under action of gamma-aminobutyric acid. *J. Neurophysiol.* **23**, 505–515.

HUSMARK, I. & OTTOSON, D. (1971). Is the adaptation of the muscle spindle of ionic origin? *Acta physiol. scand.* **81**, 138–140.

KLIE, J. W. & WELLHÖNER, H. H. (1973). Voltage clamp studies on the stretch response in the neuron of the slowly adapting crayfish stretch receptor. *Pflügers Arch.* **342**, 93–104.

KUFFLER, S. W. & EYZAGUIREE, C. (1955). Synaptic inhibition in an isolated nerve cell. *J. gen. Physiol.* **39**, 155–184.

MEYER, H. & LUX, H. D. (1974). Action of ammonium on a chloride pump. Removal of hyperpolarizing inhibition in an isolated neuron. *Pflügers Arch.* **350**, 185–195.

MILLECCHIA, R. & MAURO, A. (1969). The ventral photoreceptor cells of *Limulus*. III. A voltage-clamp study. *J. gen. Physiol.* **54**, 331–351.

NAKAJIMA, S. & ONODERA, K. (1969). Membrane properties of stretch receptor neurons of crayfish with particular reference to mechanisms of sensory adaptation. *J. Physiol.* **200**, 161–185.

OBARA, S. (1968). Effects of some organic cations on generator potential of crayfish stretch receptor. *J. gen. Physiol.* **52**, 363–386.

OTTOSON, D. (1964). The effect of sodium deficiency on the response of the isolated muscle spindle. *J. Physiol.* **171**, 109–118.

OTTOSON, D. & HUSMARK, I. (1971). Impulse activity of the isolated spindle in potassium-free solution. *Acta physiol. scand.* **83**, 486–494.

OZAWA, S. & TSUDA, K. (1973). Membrane permeability change during inhibitory transmitter action in crayfish stretch receptor cell. *J. Neurophysiol.* **36**, 805–816.

SAUNDERS, J. H. & BROWN, H. MACK (1977). Liquid and solid-state $Cl^-$-sensitive microelectrode characteristics and application to intracellular $Cl^-$ activity in *Balanus* photoreceptor. *J. gen. Physiol.* **70**, 507–530.

STRICKHOLM, A. & WALLIN, B. G. (1965). Intracellular chloride activity of crayfish giant axons. *Nature, Lond.* **208**, 790–791.

TERZUOLO, C. & WASHIZU, Y. (1962). Relation between stimulus strength, generator potential and impulse frequency in stretch receptor of crustacea. *J. Neurophysiol.* **25**, 56–66.